Desalination and Water Treatment
www.deswater.com

doi: 10.5004/dwt.2017.20200

63 (2017) 275–282
February

Decolorization of methylene blue by an attapulgite-based heterogeneous Fenton catalyst: process optimization

Ting Zhang*, Minmin Chen, Shurong Yu

Department of Petrochemical Engineering, Lanzhou University of Technology, Lanzhou, 730050, China,
Tel. 086-931-7823126; emails: zhangting@lut.cn (T. Zhang), 2550347292@qq.com (M. Chen), yusr@lut.cn (S. Yu)

Received 14 March 2016; Accepted 27 August 2016

ABSTRACT

Attapulgite (ATP)-based Fenton catalyst (Fe_2O_3/ATP) was studied during the decolorization of non-biodegradable dye methylene blue (MB). We achieved such goal by performing several batch degradation experiments under various conditions, including different pHs, Fe_2O_3/ATP and H_2O_2 dosages and the initial MB concentrations. Results revealed that relatively high decolorization efficiency (more than 99%) can be achieved in only 10 min at an initial MB concentration of 100 mg/L and temperature of 60°C. Response surface methodology (RSM) was applied with a Box–Behnken design to a series of experiments. The order of influence of the factors tested was pH > Fe_2O_3/ATP dosage > H_2O_2 dosage. By RSM, a mathematical model was established, and optimal conditions were determined.

Keywords: Attapulgite-based catalyst; Heterogeneous reaction; Methylene blue; Process optimization; Response surface methodology (RSM)

1. Introduction

Recently, several studies have been conducted to explore heterogeneous catalysts adopted for the substitution of deliquescent Fe(II) reagents of traditional homogeneous Fenton systems. Such works were formulated because the ferric ion is a kind of secondary pollutant and requires a large amount of chemicals and manpower to remove from treated water. Heterogeneous Fenton-like systems can also overcome another drawback of homogeneous Fenton systems, that is, the tight pH range. Heterogeneous Fenton-like reactions on solid catalysts can effectively catalyze the oxidation of organic pollutants at wide pH conditions, which is beneficial for the in situ remediation of polluted groundwater and soil [1].

Several kinds of heterogeneous Fenton catalysts have been studied. Tian et al. [2] and Ji et al. [3] successfully prepared iron compounds, $Fe_2(MoO_4)_3$ and $LiFe(WO_4)_2$ separately as heterogeneous Fenton-like catalysts to degrade dyes, such as Acid Orange II (AOII) and methylene blue (MB), in aqueous solution. Matta [1], Yu [4], Sun [5] and Giraldi [6] used iron-bearing earth materials and iron oxide minerals, such as ferrihydrite, hematite, goethite, lepidocrocite, magnetite, pyrite and schorl as heterogeneous Fenton catalysts to decolorize the dyes. Iron oxide minerals attract more attention for their wide spreading in the natural environment, being easily applied to in situ remediation processes. The iron-bearing catalysts or those loaded with irons can be reused for further runs and extend the pH range for Fenton oxidants. Some researchers were concerned about introducing Fe or Fe(II) or Fe(III) into porous materials (zeolite, activated carbon and activated aluminum oxide) or clays (montomorillonite, kaoline and attapulgite [ATP]) [7–16] to lower the treatment cost of waste water. For example, Feng et al. [11] studied the discoloration and mineralization of an azo dye Orange II using a bentonite-clay-based Fe-nano-composite (Fe-B) film as a heterogeneous photo-Fenton catalyst in the presence of UV-C light and H_2O_2. Hassan et al. [12] carried

---

* Corresponding author.

1944-3994/1944-3986

out a study of the decolorization of azo dye Acid Red 1 (AR1) in an aqueous solution using Fe–zeolite Y type (Fe–ZYT) catalyst. B. Muthukumari et al. [13] studied photo-assisted Fenton mineralization of two azo dyes, Direct Red 23 (DR23) and Reactive Orange 4 (RO4) in detail using an Fe(II)-loaded Al_2O_3 as a heterogeneous catalyst in the presence of H_2O_2 and UV-A light. Zhong et al. [14] prepared iron-containing mesostructured silica (Fe_2O_3/SBA-15) and used the material as heterogeneous catalyst in the integrated sono–photo-Fenton process.

Along with research on various heterogeneous Fenton catalysts, researchers are paying increased attention to the catalytic degradation process and process optimization of heterogeneous catalytic systems in degrading hard-to-degrade organics. For instance, Sun et al. [5] investigated the heterogeneous Fenton-like reactions on nano-magnetite (Fe_3O_4) for the degradation of p-nitrophenol (p-NP), and its process optimization, kinetics and degradation pathways. A four-factor central composite design (CCD) coupled with response surface methodology (RSM) was applied to evaluate and optimize the important variables. The optimum conditions were determined to be 1.5 $g\cdot L^{-1}$ Fe_3O_4, 620 mM H_2O_2, pH 7.0 and 25–45 $mg\cdot L^{-1}$ p-NP. Chen et al. [17] studied the decolorization of azo dye Orange II using a montomorillonite/H_2O_2 system and a heterogeneous Fenton system. RSM was applied with a Box–Behnken design (BBD) of a series of experiments, and results showed that the order of influence of the different factors tested was pH > KSF dosage > H_2O_2 dosage. We established a mathematical model and determined optimal conditions by RSM.

Among the promising clays, ATP clay is widely used in various processes because of ATP's crystalline, hydrated magnesium aluminum silicate exhibiting a unique three-dimensional structure, fibrous morphology and reactive –OH groups on its surface. ATP is less sensitive to salts than are other clays. Given its special layer structure, chain structure and good absorption, ATP has received considerable attention as regards its role as substrate for super absorbent composite materials and support for catalysts [18–21]. In our previous work, we investigated the catalytic Fe_2O_3/ATP in a Fenton system during degrading sodium dodecyl benzene sulfonate (SDBS), decolorizating MB and Congo red (CR) [22,23].We found that Fe_2O_3/ATP possessed a high catalytic reactivity at a wider pH range and repeated usage than in the other substances tested. When introducing ATP to Fe_2O_3, the degradation ratios of the catalysts were greatly enhanced because of ATP's excellent auxiliary catalytic ability.

In the present study, MB was also employed as a model dye compound. A series of experiments on MB degradation by a Fe_2O_3/ATP/H_2O_2 system was studied in detail. We employed RSM to optimize related parameters and analyzed the degree of importance of each factor. This study can enhance the general understanding on the catalytic process of Fe_2O_3/ATP in a heterogeneous Fenton system.

2. Experimental

2.1. Materials

ATP clay was obtained from the Xuyi county, Jiangsu Province, China (specific surface area of 146–210 m^2/g), with ATP content of 60%–70%, hydromica and montmorillonite content of 15%–28%, dolomite and quartz content of 10%–20%. Its chemical components (%) are as follows: SiO_2, 57.006; TiO_2, 0.893; Al_2O_3, 8.583; Fe_2O_3, 4.641; SO_3, 0.007; MnO, 0.034; MgO, 8.456; CaO, 0.216; K_2O, 0.094; and Na_2O, 0.948.

MB ($C_{16}H_{18}ClN_3S$, analysis purity) was purchased for use as target pollutant. The $Fe(NO_3)_3$, H_2O_2 (30%), NaOH and HCl supplied by corresponding manufacturers were analytically pure.

2.2. Decolorization and analysis methods

MB, a common cationic dye (molecular weight: 373.90), was selected as model pollutant. Its structure is shown in Fig. 1. A stock solution containing MB (1,000 mg/L) was prepared using distilled water and subsequently diluted to the required concentrations for our experimental work. Fe_2O_3/ATP particles (3 mm) were prepared by the incipient wetness technique [23]. Fe_2O_3/ATP catalyst samples were added to 100 mL of MB concentrations in conical flasks. Then, the pH was adjusted by addition of NaOH or H_2SO_4 to the dye solutions, and H_2O_2 was added. The conical flask was sealed and placed in a constant-temperature water bath. The MB concentration was measured by MB spectrophotometry using an INESA 752N type UV–visible spectrophotometer at $\lambda = 664$ nm.

2.3. Experimental design and data analysis by RSM

The BBD is an extensively used, three-level, incomplete factorial design. Seventeen experimental runs of BBD were performed to optimize the initial reaction rate and the derivative of the initial portion of the kinetic curve and to arrange in order of importance the various influencing factors tested. Table 1 shows the BBD matrix for the three variables pH, Fe_2O_3/ATP dosage and H_2O_2 dosage. The experimental data were analyzed using Design Expert 8.0.6.1 software and were fitted to a second-order polynomial equation. The optimized parameters for maximizing the initial rate were also obtained using the established equation.

2.4. Repeated decolorization experiments

To test the stability of Fe_2O_3/ATP as a catalyst and to explore the possibility of recycling, repeated decolorization experiments were performed at least 10 times. To guarantee that the initial concentrations of MB and H_2O_2 were the same for all runs, 100 mg/L of MB and 9.8 mmol/L of H_2O_2 were added to the conical flask containing 0.5 g Fe_2O_3/ATP catalyst for every run. The Fe_2O_3/ATP catalysts for each run were washed by distilled water. The experimental and analytical

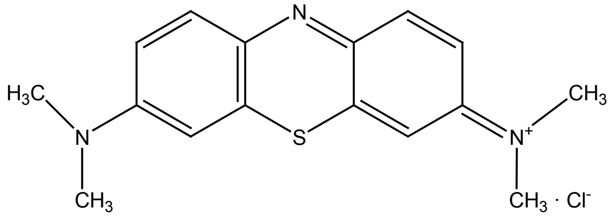

Fig. 1. Structure of methylene blue.

Table 1
Box–Behnken design for the three variables together with the observed and predicted responses

Experimental run	Coded variables		
	pH (X_1)	H_2O_2 dosage (X_2, mmol/L)	Fe_2O_3/ATP dosage (X_3, g/L)
1	12	98	6
2	2	19.6	6
3	7	19.6	2
4	2	58.8	2
5	7	98	10
6	7	58.8	6
7	2	98	6
8	7	19.6	10
9	7	58.8	6
10	7	98	2
11	12	19.6	6
12	7	58.8	6
13	7	58.8	6
14	12	58.8	10
15	7	58.8	6
16	2	58.8	10
17	12	58.8	2

methods for each run were the same as that for the oxidation reaction and analysis mentioned above.

3. Results and discussion

3.1. Comparison experiment

Setting the initial concentration of MB at 100 mg/L and pH at 2, the efficiency for the decolorization of MB by adding 5 g/L of Fe_2O_3/ATP and 9.8 mmol/L of H_2O_2 was investigated.

To gain an insight into the process of the MB decolorization by Fe_2O_3/ATP/H_2O_2 system, comparative experiments were undertaken in the presence of (i) H_2O_2 only, (ii) Fe_2O_3/ATP only and (iii) both Fe_2O_3/ATP and H_2O_2. The results are displayed in Fig. 2. Fig. 2(a) displays that at room temperature, the decolorization ratio of MB is not extremely high when only H_2O_2 exists and merely obtains 20% decolorization ratio after 24 h. When only Fe_2O_3/ATP exists, the decolorization ratio of MB can reach over 60% after 24 h. This result may be due to the adsorptive ability of Fe_2O_3/ATP or the catalytic reaction occurring on Fe_2O_3/ATP with light and oxygen. When both Fe_2O_3/ATP and H_2O_2 exist, the decolorization ratio of MB can reach 99% in 4 h. At a high temperature of 60°C, the decolorization ratio of MB considerably fluctuated when only H_2O_2 existed; the ratio rose then declined and obtained an 80% decolorization ratio at 60 min (Fig. 2(b)). This finding can be explained by the notion that MB can be oxidized by H_2O_2 and generate an intermediate product of high chromaticity. Such intermediate can then be partially oxidized by H_2O_2 gradually, and the decolorization ratio increases but not substantially. When only Fe_2O_3/ATP was present at 60°C, the decolorization ratio was extremely low because of the high temperature and short contact time. When both Fe_2O_3/ATP and $H_2O_2$was present at 60°C, the decolorization ratio of MB can reach 99% in 10 min.

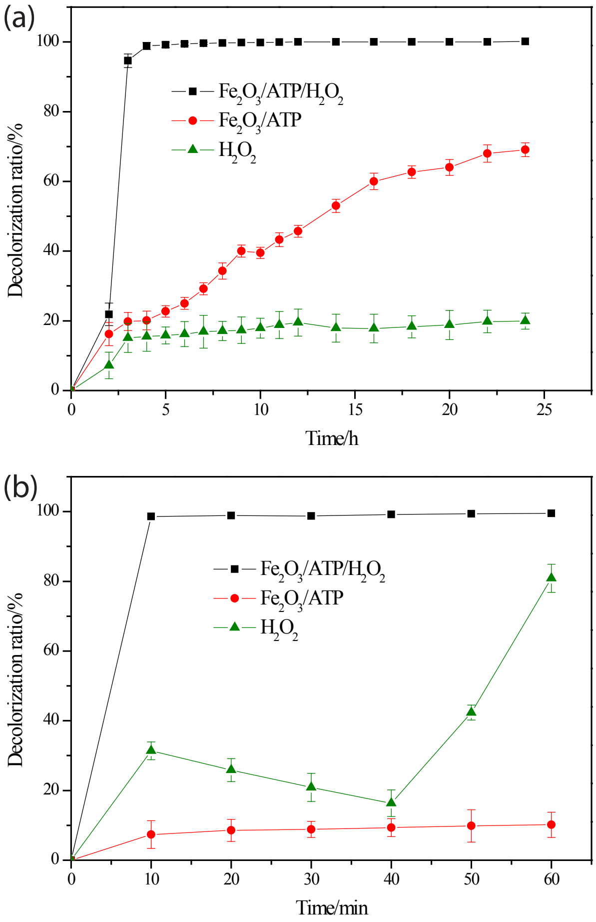

Fig. 2. Comparison of MB decolorization versus time among different temperatures (a) at 25°C and (b) at 60°C.

Fe_2O_3/ATP exhibited good adsorption of MB (Fig. 2), and some experiments on adsorption isotherms were conducted (Fig. 3). The isotherm was fitted with the Langmuir equation, and results showed that the process of Fe_2O_3/ATP adsorption of MB attained a good fit because of the high R value (R = 0.999).

According to literature [24] and Table 2, H_2O_2 is highly stable and will not decompose at temperatures below 35°C. At 60°C, the H_2O_2 decomposition ratio was only 0.67%. Under 90°C, the H_2O_2 decomposition ratio was not extremely high. These results reveal that the experimental temperatures we adopted were feasible and slightly influenced H_2O_2 decomposition. Meanwhile, high temperature was observed to greatly improve the catalytic and decolorizing efficiency.

3.2. Effect of pH on MB decolorization

The decolorization of MB in aqueous solution in the presence of Fe_2O_3/ATP was studied in the pH range between 2 and 12. Table 3 shows the decolorization efficiency of MB after 60 min at different pH values using an initial solution containing 100 mg/L MB, 5 g/L catalyst and 4.9 mmol/L H_2O_2. Almost complete decolorization was achieved at pH 2

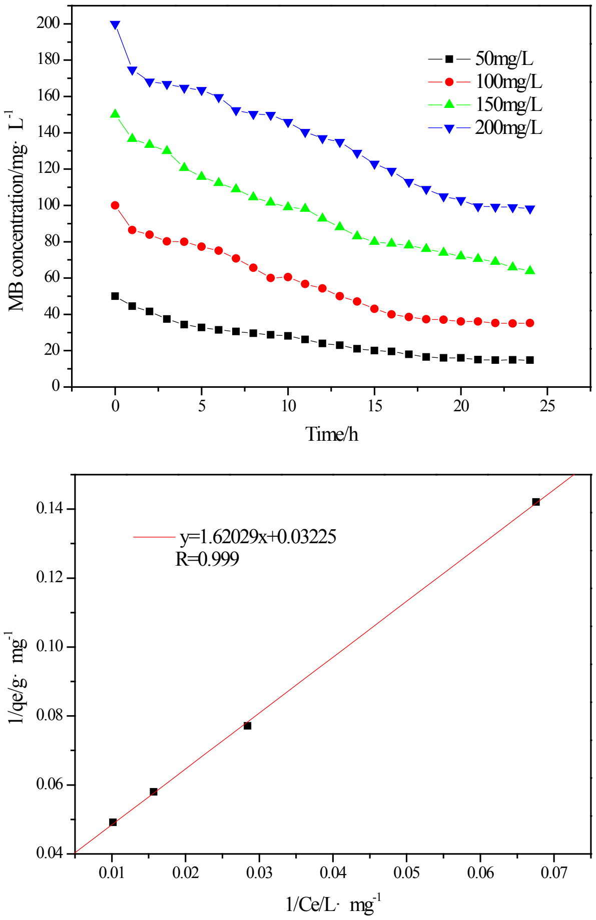

Fig. 3. MB adsorption at different initial concentrations by Fe_2O_3/ATP at 25°C.

Table 2
Relationship between temperature and H_2O_2 decomposition ratio

Temperature (°C)	H_2O_2 decomposition ratio (η, %)
30	0
40	0.16
50	0.61
60	0.67

(99.56%) and pH 4 (98.95%) (Table 3). At pH 6, 8, 10 and 12, 40.91%, 40.84%, 35.85% and 20.88% decolorization ratios were obtained, respectively. Some researchers reported that the stability of H_2O_2 was dependent on pH value. H_2O_2 did not decompose at pH < 3.5 and presented with relatively low decomposition ratios in acidic pH. In the presence of catalysts, most of the H_2O_2 was transformed to OH radicals. At neutral and alkaline pH conditions, H_2O_2 decomposition ratios were extremely high, reaching about 60%–80% H_2O_2 decomposed and O_2 released. Only a small portion of H_2O_2 was catalyzed and produced OH radicals (Table 4) [25]. The oxidation potential of OH radicals was shown to be lower in alkaline than in acidic conditions [5]. OH radicals achieve a stronger oxidation at acidic conditions than at neutral and alkaline conditions.

Table 3
Effect of individual variables on the decolorization efficiency after 60 min

Variables			Decolorization efficiency (%)
pH	Fe_2O_3/ATP dosage (g/L)	H_2O_2 dosage (mmol/L)	
2	5	4.9	99.56
4	5	4.9	98.95
6	5	4.9	40.91
8	5	4.9	40.84
10	5	4.9	35.85
12	5	4.9	20.88
2	1	4.9	97.18
2	3	4.9	99.51
2	5	0.98	1.35
2	5	1.47	90.61
2	5	1.96	93.24
2	5	3.92	99.50
2	5	9.8	99.01
2	5	19.6	99.72
2	5	39.2	99.82

Table 4
Relationship between decomposition ratio of H_2O_2 and pH value

pH	Decomposition ratio of H_2O_2 (η, %)
3.10	1.0
4.13	1.2
5.09	2.6
5.30	5.6
5.50	12.1
6.22	20.9
6.33	40.0
6.55	55.2
7.00	62.8
8.00	80.0
9.00	86.0
9.03	86.1
10.10	74
11.20	67.3
12.00	61.9

3.3. Effect of Fe_2O_3/ATP dosage on MB decolorization

An increase in MB decolorization efficiency was noted with an increase in Fe_2O_3/ATP dosage and experimental conditions of 100 mg/L MB, 4.9 mmol/L H_2O_2 and pH 2 (Table 3). This phenomenon illustrates that an increase in Fe_2O_3/ATP dosage favored the enhancement of MB decolorization. Results of a series of experiments indicated that MB decolorization efficiency slightly decreased at a Fe_2O_3/ATP dosage of 3 g/L and even 1 g/L in contrast with 5 g/L. A sufficient amount of Fe_2O_3 active sites were present on ATP even at low dosages and can catalyze H_2O_2, still consequently yielding high decolorization efficiency.

3.4. Effect of H_2O_2 dosage on MB decolorization

The influence of H_2O_2 concentration on MB decolorization is also investigated and presented in Table 3. H_2O_2 concentration varied from 0.98 mmol/L to 39.2 mmol/L with experimental conditions of 100 mg/L MB, 5 g/L Fe_2O_3/ATP dosage and pH 2. The results show that MB decolorization ratio was heavily dependent on H_2O_2 concentration. Only a 1.35% decolorization ratio was achieved when the H_2O_2 concentration was 0.98 mmol/L, and a slight increase in H_2O_2 concentration (1.47 mmol/L) led to a high decolorization efficiency (90.61%). We deduce the presence of a breakthrough point between 0.98 mmol/L to 1.47 mmol/L for the MB decolorization. Before this breakthrough point, no OH was produced. Only after this breakthrough point, OH was produced, and the catalysis reaction was effective. Over 90% decolorization ratios were achieved when H_2O_2 concentration changed from 1.47 mmol/L to 39.2 mmol/L. This observation can be explained by the fact that H_2O_2 does not decompose into H_2O and O_2 at pH 2, but transforms to·OH completely when catalyzed by Fe_2O_3/ATP. Furthermore, the OH decomposed from only a slight amount of H_2O_2 (1.47 mmol/L) that can oxidize and fade the chromogenic groups of MB. We can also see that when H_2O_2 concentration varied from 3.92 mmol/L to 39.2 mmol/L, the decolorization ratios almost remained the same, indicating that 3.92 mmol/L H_2O_2 was sufficient to decolorize 100 mL, 100 mg/L of MB, and increasing H_2O_2 does not directly result in big augmented decolorization ratio.

3.5. Experimental design, data analysis and optimization by RSM

The data of 17 experimental runs using the BBD were analyzed using Design Expert 8.0.6.1 software and were fitted to a second-order polynomial equation. The function presented below was employed as the prediction model:

$$\begin{aligned} Y = {} & 58.06343 - 1.97448X_1 + 1.13259X_2 + 52.8675X_3 \\ & + 0.020867X_1X_2 + 7.4425X_1X_3 - 0.21186X_2X_3 \\ & - 0.77118X_1^2 - 8.78E - 03X_2^2 - 36.94688X_3^2 \end{aligned}$$

where Y is the decolorization ratio of MB (%), X_1 is the pH (2–12), X_2 is the H_2O_2 concentration (19.8–98 mmol/L), and X_3 is the Fe_2O_3/ATP dosage (1–10 g/L). Analysis of variance (ANOVA) was used to test the significance and adequacy of the model, giving a correlation coefficient of $R^2 = 0.9834$ (Table 5).

ANOVA analysis indicated that the calculated F value of 46.1 was much larger than the critical value of 3.68 for $F_{0.05}$ (9, 7). This information implies that the derived quadratic polynomial model was significant. In addition, the model correlation coefficient of $R^2 = 0.9834$ suggests the good agreement between the experimental and predicted values of the degradation efficiency of MB. The predicted decolorization

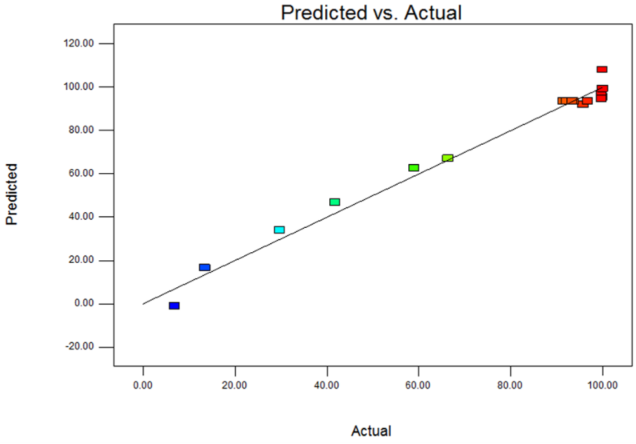

Fig. 4. Comparison of the model-predicted decolorization efficiencies of MB and experimental values.

Table 5
ANOVA results of the quadratic model of the decolorization ratio

Source	Sum of squares	Degree of freedom	Mean square	*F* value	*p*-value (prob > *F*)	
Model	16,868.97	9	1,874.33	46.1	<0.0001	Significant
X_1 (pH)	10,021.03	1	10,021.03	246.46	<0.0001	
X_2 (H_2O_2 concentration)	173.05	1	173.05	4.26	0.078	
X_3 (catalyst dosage)	2,970.2	1	2,970.2	73.05	<0.0001	
$X_1 \cdot X_2$	66.91	1	66.91	1.65	0.2404	
$X_1 \cdot X_3$	886.25	1	886.25	21.8	0.0023	
$X_2 \cdot X_3$	44.14	1	44.14	1.09	0.3321	
X_1^2	1,565.05	1	1,565.05	38.49	0.0004	
X_2^2	766.97	1	766.97	18.86	0.0034	
X_3^2	147.14	1	147.14	3.62	0.0989	
Residual	284.61	7	40.66			
Lack of fit	268.28	3	89.43	21.89	0.0061	Significant
Pure error	16.34	4	4.08			
Corrected total	17,153.58	16				

Note: $R^2 = 0.9834$; adjusted $R^2 = 0.9621$.

efficiency of MB agrees well with the experimental values (Fig. 4). The derived model was adequate in performing the process variable optimization for the decolorization of MB. The significance of each independent variable was evaluated in accordance with its P-value of 0.0061, which was lower than 0.05, signifying that the term was significant at 95% confidence level. The results indicate that the decolorization efficiency of MB was significantly affected by catalyst dosage, initial H_2O_2 concentration and initial pH.

Fig. 5 shows the response surface modeling in the 3D representation of the effects of catalyst dosage, initial H_2O_2 concentration and the initial pH on the decolorization of MB by heterogeneous Fenton-like reactions on Fe_2O_3/ATP. Figs. 5(a) and 5(b) show that pH is a crucial operating parameter for the Fe_2O_3/ATP/H_2O_2 system in MB decolorization, directly affecting the catalytic performance. Along with increasing pH value, MB decolorization decreased rapidly, even at a relatively high H_2O_2 concentration and catalyst dosage. This result can be explained by the fact that neutral and basic conditions provide more hydrogen peroxide to decompose into O_2 and H_2O, while not generating OH. The optimum dosages of hydrogen peroxide and catalyst increased with initial pH rise (Fig. 5(a) and 5(b)). In Fig. 5c, H_2O_2 concentration and catalyst dosage slightly influenced MB decolorization ratio, whereas the overall trend suggested that higher catalyst dosage and moderate H_2O_2 concentration generated a high MB decolorization. Excessive H_2O_2 levels resulted in a slight decrease in MB decolorization ratio because H_2O_2 reacted with OH.

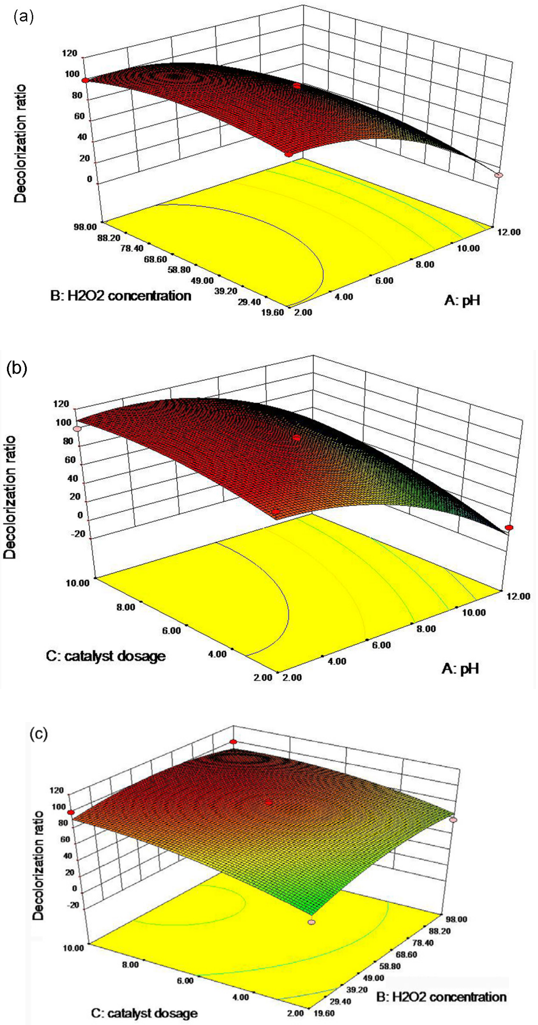

Fig. 5. 3D response surface and contour plots of the MB decolorization ratio.

3.6. *Effect of MB initial concentration*

The effect of initial MB concentration on its decolorization was also investigated. The experimental conditions are the H_2O_2 concentration of 9.8 mmol/L, Fe_2O_3/ATP dosage of 5 g/L, pH value of 3, temperature of 60°C and the initial MB concentration from 50 mg/L to 200 mg/L. The results are shown in Fig. 6 and indicate that the decolorization efficiency at 50 mg/L MB was not obviously higher than at 200 mg/L MB. The decolorization after 40 min was 97.19% at 50 mg/L and 96.19% at 200 mg/L. Even after 60 min, the decolorization efficiency at 50 and 200 mg/L reached 99.04% and 98.31%, respectively. Meanwhile, during the decolorization of high concentrations (150 and 200 mg/L) of MB, the obvious phenomena of color reversion was observed. We thus conclude that during the OH oxidation of MB, an intermediate product with high chromaticity was produced, and this intermediate was oxidized by OH. This color reversion phenomena also occurred during the decolorization of low concentrations (50 and 100 mg/L) of MB, but the production and oxidation of the high-chromaticity intermediate in this case took place excessively fast to be detected.

To investigate the kinetics, we used three models, namely, first-order, second-order and the Langmuir–Hinshelwood (L–H) equations, to describe our experimental data. The results are presented in Table 6. By comparing the R^2 value for each equation, we concluded that the L–H equation achieved the best fit. The R^2 values for first-order, second-order and L–H equations were 0.9034, 0.8367 and 0.9833, respectively. Given these data, we chose the Langmuir–Hinshelwood (L–H) equation to describe MB decolorization for the concentration range of 50 mg/L to 200 mg/L.

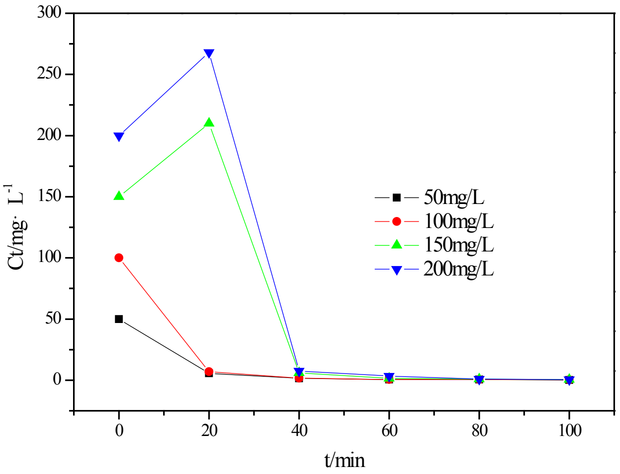

Fig. 6. MB degradation vs. time at different initial concentrations under 60°C.

Table 6
Kinetics analysis of MB decolorization

Model	Kinetics equation	k (mg/L·min)	R^2	K (L/mg)
First-order	$r = 0.052C$	0.052	0.9034	
Second-order	$r = 0.0479C^2$	0.0479	0.8367	
L–H model	$r = \dfrac{0.046C}{1+0.001012C}$	45.457	0.9833	0.001012

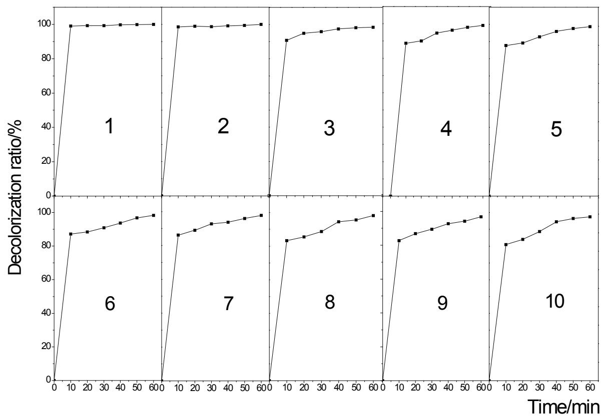

Fig. 7. Ten-times repeated decolorization experiments.

3.7. Repeat decolorization experiments

Ten-times repeated decolorization experiments were performed to test the stability of Fe_2O_3/ATP as catalyst (Fig. 7). After the first run, the decolorization efficiency of MB was 99.9%. In subsequent runs, the decolorization efficiency decreased but not excessively. At the end of the fifth and tenth runs, the efficiency was 98.65% and 97.39%, respectively. The experiments showed that catalyst Fe_2O_3/ATP did not lose its catalytic function after several runs, suggesting that the catalyst did not lose its active Fe(III) from the catalyst surface. For practical application, how many runs by which Fe_2O_3/ATP can catalyze and degrade organic pollutants while maintaining high efficiency is worth further investigation. The resultant data could promote the wider application of Fe_2O_3/ATP as a catalyst for the Fe_2O_3/ATP/H_2O_2 system and other wastewater treatment processes.

4. Conclusions

MB was successfully decolorized in water by the heterogeneous catalytic decomposition of hydrogen peroxide on Fe_2O_3/ATP. With the coating iron species on the ATP surface, the materials provided a sufficient number of active sites to support heterogeneous Fenton reactions and exhibited remarkable catalytic performance. The MB degradation performances by Fe_2O_3/ATP, H_2O_2 and Fe_2O_3/ATP/H_2O_2 under different temperatures were studied. The experimental results demonstrated in the presence of H_2O_2 or Fe_2O_3/ATP alone that the MB decolorization ratio was not considerably high. By contrast, under the presence of both H_2O_2 and Fe_2O_3/ATP in solution, the decolorization efficiency reached as high as 99% after 5 h under 25°C and after 10 min under 60°C.

Furthermore, the results indicated that BBD coupled with RSM is a useful technique for optimizing the important parameters of heterogeneous Fenton-like reactions on Fe_2O_3/ATP for MB degradation. The order of influence of the different factors studied was pH > Fe_2O_3/ATP dosage > H_2O_2 dosage. Moreover, the model predicted that the optimal conditions were pH 3, 10 g/L Fe_2O_3/ATP and 58.8 mmol/L H_2O_2. At pH 3 and initial concentrations of 50 mg/L to 200 mg/L, the decolorization of MB followed the L–H equation. The Fe_2O_3/ATP catalyst was reused for more than 10 times. Given the experiments, we found that Fe_2O_3/ATP-catalyzed Fenton-like systems hold the unique advantages of easy separation from treated wastewater, high catalytic reactivity at a wide pH range, recyclability and absence of secondary pollutants.

Acknowledgment

This work was financially supported by the National Natural Science Foundation of China (Grant No. 51302123).

References

[1] R. Matta, K. Hanna, S. Chiron, Fenton-like oxidation of 2,4,6-trinitrotoluene using different iron minerals, Sci. Total Environ., 385 (2007) 242–251.

[2] S.H. Tian, Y.T. Tu, D.S. Chen, X. Chen, Y. Xiong, Degradation of Acid Orange II at neutral pH using $Fe_2(MoO_4)_3$ as a heterogeneous Fenton-like catalyst, Chem. Eng. J., 169 (2011) 31–37.

[3] F. Ji, C.L. Li, J.H. Zhang, L. Deng, Heterogeneous photo-Fenton decolorization of methylene blue over $LiFe(WO_4)_2$ catalyst[J], J. Hazard. Mater., 186 (2011) 1979–1984.

[4] H.Y. YU, M. Prasad, X.L. He, L.W. Shan, S.Y. Qi, Discoloration of Rhodamine B dyeing wastewater by schorl-catalyzed Fenton-like reaction, Sci. China Series E: Technol. Sci., 52 (2009) 3054–3060.

[5] S.P. Sun, A.T. Lemley, P-Nitrophenol degradation by a heterogeneous Fenton-like reaction on nano-magnetite: process optimization, kinetics, and degradation pathways, J. Mol. Catal. A: Chem., 349 (2011) 71–79.

[6] T.R. Giraldi, C.C. Arruda, G.M. da Costa, E. Longo, C. Ribeiro, Heterogeneous Fenton reactants: a study of the behavior of iron oxide nano particles by the polymeric precursor method, J. Sol-Gel Sci. Technol., 52 (2009) 299–303.

[7] J. Feng, X. Hu, P.L. Yue, Novel bentonite clay-based Fe nanocomposite as a heterogeneous catalyst for photo-Fenton discoloration and mineralization of Orange II, Environ. Sci. Technol., 38 (2004) 269–275.

[8] J. Feng, X. Hu, P.L. Yue, Discoloration and mineralization of Orange II using different heterogeneous catalysts containing Fe: a comparative study, Environ. Sci. Technol., 38 (2004) 5773–5778.

[9] J.X. Chen, L.Z. Zhu, Catalytic degradation of Orange II by UV-Fenton with hydroxyl-Fe-pillared bentonite in water, Chemosphere, 65 (2006) 1249–1225.

[10] J.X. Chen, L.Z. Zhu, Oxalate enhanced mechanism of hydroxyl-Fe-pillared bentonite during the degradation of Orange II by UV-Fenton process, J. Hazard. Mater., 185 (2011) 1477–1481.

[11] J.Y. Feng, X.J. Hu, P.L. Yue, Discoloration and mineralization of Orange II by using abentonite clay-based Fe nanocomposite film as a heterogeneous photo-Fenton catalyst, Water Res., 39 (2005) 89–96.

[12] H. Hassan, B.H. Hameed, Oxidative decolorization of Acid Red 1 solutions by Fe–zeolite Y type catalyst, Desalination, 276 (2011) 45–52.

[13] B. Muthukumari, K. Selvam, I. Muthuvel, M. Swaminathan, Photoassisted hetero-Fenton mineralization of azo dyes by Fe(II)-Al_2O_3 catalyst, J. Chem. Eng., 153 (2007) 9–15.

[14] X. Zhong, S. Royer, H. Zhang, Q.Q. Huang, L.J. Xiang, S. Valange, J. Barrault, Mesoporous silica iron-doped as stable and efficient heterogeneous catalyst for the degradation of C.I. Acid Orange 7 using sono-photo-Fenton process, Separ. Purif. Technol., 80 (2011) 163–171.

[15] S.S. Martínez, J.V. Sánchez, J.R.M. Estrada, R.F. Velásquez, Fe^{III} supported on ceria as effective catalyst for the heterogeneous photo-oxidation of basic orange 2 in aqueous solution with sunlight, Solar Energy Mater. Solar Cells, 95 (2011) 2010–2017.

[16] Q.Q. Chen, P.X. Wu, Y.Y. Li, N.W. Zhu, Z. Dang, Heterogeneous photo-Fenton photodegradation of reactive brilliant orange X-GNover iron-pillared montmorillonite under visible irradiation, J. Hazard. Mater., 168 (2009) 901–908.

[17] L. Chen, C.Y. Deng, F. Wu, N.S. Deng, Decolorization of the azo dye Orange II in a montmorillonite/H_2O_2 system, Desalination, 281 (2011) 306–311.

[18] L. Wang, J. Sheng, Preparation and properties of polypropylene/org-attapulgite nanocomposites, Polym., 46 (2005) 6243–6249.

[19] W.S. Wu, Q.H. Fan, J.Z. Xu, Z.W. Niu, S.S. Lu, Sorption–desorption of Th(IV) on attapulgite: effects of pH, ionic strength and temperature, Appl. Radiat. Isotopes, 65 (2007) 1108–1114.

[20] J. Zhang, H. Chen, A. Wang, Study on superabsorbent composite. III. Swelling behaviors of polyacrylamide/attapulgite composite based on acidified attapulgite and organo-attapulgite, Eur. Polym. J., 41 (2005) 2434–2442.

[21] A. Li, J.P. Zhang, A.Q. Wang, Utilization of starch and clay for the preparation of superabsorbent composite, Bioresour. Technol., 98 (2007) 327–332.

[22] T. Zhang, Sodium Dodecyl Benzene Sulfonate (SDBS) degradation by heterogeneous Fenton-like reactions on two types of catalysts: experimental and comparison, Res. J. Chem. Environ., 17 (2013) 32–39.

[23] T. Zhang, Z. Nan, Decolorization of Methylene Blue and Congo Red by attapulgite-based heterogeneous Fenton catalyst, Desal. Wat. Treat., 57 (2016) 4633–4640.

[24] Z.X. Liu, C.X. Xie, N. Shi, W. Xu, Properties research of hydrogen peroxide decomposition, Petrochem. Technol., 37 (2009) 99–102.

[25] Z.Z. Xu, X.C. Li, Analysis of factors affecting hydrogen peroxide decomposition, Dye. Finish. Technol., 28 (2006) 33–35.